Extremophiles (2003) 7:483–491
DOI 10.1007/s00792-003-0348-1

ORIGINAL PAPER

Maher Abou-Hachem · Fredrik Olsson
Eva Nordberg Karlsson

Probing the stability of the modular family 10 xylanase from *Rhodothermus marinus*

Received: 13 March 2003 / Accepted: 7 July 2003 / Published online: 26 August 2003

Abstract The thermophilic bacterium *Rhodothermus marinus* produces a modular xylanase (Xyn10A) consisting of two N-terminal carbohydrate-binding modules (CBMs), followed by a domain of unknown function, and a catalytic module flanked by a fifth domain. Both Xyn10A CBMs bind calcium ions, and this study explores the effect of these ions on the stability of the full-length enzyme. Xyn10A and truncated forms thereof were produced and their thermostabilities were evaluated under different calcium loads. Studies performed using differential scanning calorimetry showed that the unfolding temperature of the Xyn10A was significantly dependent on the presence of Ca^{2+}, and that the third domain of the enzyme binds at least one Ca^{2+}. Thermal inactivation studies confirmed the role of tightly bound Ca^{2+} in stabilizing the enzyme, but showed that the presence of a large excess of this ion results in reduced kinetic stability. The truncated forms of Xyn10A were less stable than the full-length enzyme, indicative of module/domain thermostabilizing interactions. Finally, possible roles of the two domains of unknown function are discussed in the light of this study. This is the first report on the thermostabilizing role of calcium on a modular family 10 xylanase that displays multiple calcium binding in three of its five domains/modules.

Keywords Calcium binding · CBM · Modular xylanase · Thermostable

Communicated by G. Antranikian

M. Abou-Hachem · F. Olsson · E. Nordberg Karlsson (✉)
Department of Biotechnology,
Center for Chemistry and Chemical Engineering,
Lund University, P.O. Box 124, 221 00 Lund, Sweden
E-mail: eva.nordberg_Karlsson@biotek.lu.se
Tel.: +46-46-2224626
Fax: +46-46-2224713

Introduction

The cell wall of terrestrial plants is a composite material in which cellulose microfibrils are embedded in an amorphous matrix of hemicellulose, intimately associated with lignin either covalently or noncovalently (Tomme et al. 1995). Xylan, the major component of hemicellulose, is a structurally complex polysaccharide comprised of a homopolymeric backbone of β-(1 $\rightarrow$ 4) linked D-xylopyranose with a variety of substituents and degrees of substitution depending on its origin (Joseleau et al. 1992). In marine environments, other sources for xylan exist such as red algae known to produce β-(1 $\rightarrow$ 4) and β-(1 $\rightarrow$ 3) mixed linkage xylan (Painter 1983). An ensemble of hydrolases that act in concert and synergistically is required to exploit this abundant substrate. Hence, glycoside-hydrolase multiplicity is a common theme among complex polysaccharide degraders, and aerobic microorganisms typically produce numerous extracellular individual hydrolytic enzymes, including xylanases to elicit efficient degradation (Gilbert and Hazlewood 1993; Tomme et al. 1995). These glycoside hydrolases (GHs) are typically modular in organization consisting of catalytic modules (CMs) joined to noncatalytic modules (NCMs) usually, but not always, by flexible linker sequences (Tomme et al. 1995; Warren 1996). Ancillary carbohydrate binding modules (CBMs) are the most common NCMs, but a plethora of other domains or modules have been reported. These include modules involved in cell adhesion, cellulosomal assembly, or protein anchoring (Coutinho and Henrissat 1999). The CBMs have been classified into families (currently 32 according to the CAZY server; http://afmb.cnrs-mrs.fr/~cazy/CAZY/index.html) based on primary structure similarities with members of the same family sharing a common fold. In the same system, glycoside hydrolases have been classified into families sharing primary structure, 3-D fold, and stereospecificity (Coutinho and Henrissat 1999; Henrissat et al. 1998). Xylan-degrading enzymes are clustered into the

glycoside hydrolase families (GHFs) 10 and 11. Family 10 xylanases consist of TIM-barrel folded CMs (>30 kDa) often associated with other catalytic or auxiliary modules to form large enzymes up to 120 kDa (Fujimoto et al. 2000; Sunna et al. 2000). Although the number of reported modular GHs has shown a rapid increase recently, many questions regarding their modular architecture, stability determinants, and modes of action remain unanswered.

The thermophilic marine bacterium *Rhodothermus marinus* (Alfredsson et al. 1988) produces a modular family 10 xylanase Xyn10A (Nordberg Karlsson et al. 1997). The enzyme consists of two N-terminal family 4 CBMs (Abou-Hachem et al. 2000) followed by a domain of unknown function, a catalytic module, and a C-terminal small domain. The thermal stability of the CBMs have been studied in our laboratory and we provided evidence that CBM4-2 binds two calcium ions with significantly enhanced thermostability (Abou-Hachem et al. 2002). These findings raised the question of whether the calcium thermostabilizing role was confined to the N-terminal CBMs, or if the divalent ion increased the stability of the whole modular enzyme. Furthermore, it was of interest to investigate whether module/domain interactions were critical for the stability of the enzyme or whether their presence served other important roles yet to be assigned. In an effort to address these questions, different deletion mutants of the enzyme were produced and characterized with respect to their kinetic stabilities and unfolding temperatures as well as other biochemical properties. The effects of calcium ions on stability and activity were explored. The results are discussed with respect to the modular architecture of the protein and possible roles of its two domains whose functions are yet to be ascribed.

Materials and methods

Bacterial strains and plasmids

The *Escherichia coli* strain Nova Blue was used in the cloning procedure employing the expression vector pET22b(+) under the control of a T7/lac promoter (+) (Novagen, Madison, WI). The *E. coli* strain BL21(DE3) from the same source was used as a production strain.

Cloning the different Xyn10A constructs and sequence analysis

Five different constructs, encoding either the full-length *Rhodothermus marinus* xylanase (Xyn10A) or deletion mutants thereof, were designed (Fig. 1). Standard molecular biology protocols were used throughout. The different gene fragments were amplified by PCR using *R. marinus* genomic DNA as template and Expand High Fidelity polymerase mix (Roche, Mannheim, Germany). A hot-start standard protocol consisting of an initial denaturation at 94 °C for 5 min followed by 25 cycles of denaturation at 94 °C for 30 s, 30 s of annealing at 55 °C, and 2 min extension at 68 °C was used for DNA amplification. The sequences of the different primer pairs employed for the PCR amplification are shown in Table 1. Purified vectors and PCR amplicons were double digested with appropriate restriction enzymes, separated on agarose gels, and purified using QIAEX II gel extraction kit (Qiagen, Hilden, Germany). An overnight ligation of the different constructs was followed by transformation into electrocompetent cells using a standard protocol. Plasmids were prepared from selected transformants and the presence of inserts in the correct reading frames as well as their sizes was assessed by complete nucleotide sequencing by the dideoxy chain-termination method utilizing ABI PRISM Big Dye Terminator Cycle Sequencing Ready Reaction (Perkin Elmer, Foster City, CA). Plasmids encoding the different constructs were retransformed into the production strain BL21(DE3) as described above. Several bioinformatic tools on the ExPasy server (http://expasy.ch) were used to explore the primary and secondary structure of the third and fifth domains of *Rm*Xyn10A. Similarity BLAST searches were performed on the NCBI server (http://www.ncbi.nlm.nih.gov). The ClustalW tool on the EBI server (http://www.ebi.ac.uk/clustalw) was used for multisequence alignments.

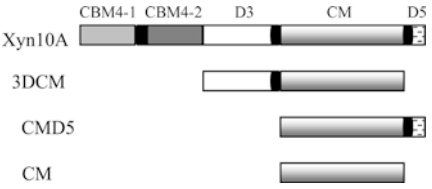

Fig. 1 Schematic representation of the different constructs characterized in this study. The full-length xylanase (*Xyn10A*, 107.6 kDa), the deletion mutants consisting of the third domain and the catalytic module (*D3CM*, 60.6 kDa), the catalytic module and the fifth domain (*CMD5*, 48.3 kDa), and the isolated catalytic module (*CM*, 37.7 kDa) were all produced in fusion with a C-terminal histidine affinity tag. The *black solid segments* denote linkers

Production and purification

Initial expression studies were carried out in 2-l baffled shake flasks and LB medium supplemented with ampicillin (0.1 g l^{-1}). Cells harboring plasmids encoding the different constructs were grown at 37 °C up to $OD_{620}=0.6$, before induction with isopropyl-β-D-thiogalactopyranoside (IPTG) to a final concentration of 1 mM, and thereafter the cultivations were continued for 3 h. To produce sufficient quantities for characterization of the xylanase constructs that displayed successful expression (evaluated by electrophoretic analysis, see below), batch cultivations were employed. Cultivation medium and control conditions during the batch phase were as outlined elsewhere (Ramchuran et al. 2002). Cells were induced at OD_{620} values between 3 and 4, and cultivations were continued for an additional 1–3 h. Cells were harvested by centrifugation at 4 °C and 10,400 *g* for 30 min. Pellets were resuspended in binding buffer (20 mM TRIS-HCl pH 7.5/20 mM imidazole/0.75 M NaCl) and stored at 4 °C for later use. Disintegration of the cells was performed using either of two techniques: (1) for volumes exceeding 1 l, cell suspensions were passed through a Gaulin high pressure homogenizer (APV-Schröder, Lübeck, Germany) in a three-cycle procedure at 500 bar or (2) pellets from shake-flask cultivation were resuspended in 50 ml binding buffer and sonicated (60 W/cm^2, 0.5 cycle, for 5×5 min) with a UP400S sonicator (Dr. Hielscher, Stahnsdorf, Germany) while cooling on an ice-water mixture. Disintegration was followed by a heat treatment step at 65 °C for 30 min and a centrifugation step for 40 min at 39,100 *g* and 4 °C for removal of cell debris and denatured aggregated proteins. The resulting supernatants were stored at 4 °C for later purification. Immobilized metal-ion affinity chromatography (IMAC) was employed to purify the produced protein as described elsewhere (Abou Hachem et al. 2000). Eluted purified proteins were dialyzed extensively against 50 mM TRIS-HCl pH 7.5 buffer and stored for later use. The construct D3CM was purified using heat treatment followed by ultrafiltration using Sartocon Micro filtration modules with a 5-kDa molecular mass cut-off (Sartorious, Göttingen,

Table 1 Primers used for cloning the different xylanase constructs. The introduced restrictions sites are *underlined*

Construct	Oligonucleotide pair
Xyn10A	F: 5′-CTATCACTCATATGCAGACGCCGGCAAATGTCAATGG-3′ R: 5′-ATATTCTCGAGCCGCATCAGCACAAGCCGG-3′
D3CM	F: 5′-CTATCACTCATATGTCGGTGGGAGCCTGGCGG-3′ R: 5′-ATTATCTCGAGGTTGGCGCTCAGGTACGACTCTCG-3′
CM	F: 5′-ATTACACTCATATGCTTGCGGCTGATGTGGATAAGTTCC-3′ R: 5′-ATTATCTCGAGGTTGGCGCTCAGGTACGACTCTCG-3′
CMD5	F: 5′-ATTACACTCATATGCTTGCGGCTGATGTGGATAAGTTCC-3′ R: 5′-ATATTCTCGAGCCGCATCAGCACAAGCCGG-3′
D3	F: 5′-CTATCACTCATATGTCGGTGGGAGCCTGGCGG-3′ R: 5′-ATATTCTCGAGTCCGCCCGTGTCCAGATCCG-3′

Germany). Protein concentrations were estimated by measuring the A_{280} and using the theoretically calculated extinction coefficients. The BCA assay (Sigma, St. Louis, MO) was also used to confirm the above concentrations using bovine serum albumin as a standard, and the two methods were in agreement. Samples to be used for the thermal inactivation studies were dialyzed against 200 vol 50 mM sodium phosphate buffer, pH 7.5, and stored at 4 °C.

Electrophoresis and activity staining

The production and purification of the different xylanase constructs were analyzed using sodium dodecyl sulfate polyacrylamide gel electrophoresis (SDS-PAGE) using 12.5% separation gels. Enzyme activity was detected by activity staining as previously described (Wicher et al. 2001), except for the following modifications: the overlayer agarose gel contained 0.05% oat spelt xylan (Sigma), the buffer used was 50 mM TRIS-HCl, pH 7.5, and the incubation time at 65 °C was 20 min. The affinity of the xylanase variants toward galactomannan and β-1,3-xylan was tested using affinity electrophoresis as previously described (Abou Hachem et al. 2000). Native polyacrylamide native gels (10%) with or without 0.1% (w/v) locust bean gum galactomannan (Sigma) or 0.2% (w/v) β-1,3-xylan from the green algae *Carelpa racemosa* (kindly provided by Professor T. Araki, Laboratory for the Utilisation of Aquatic Bioresources, Mie University, Japan) were used in the experiment.

Differential scanning calorimetry

Differential scanning calorimetry (DSC) measurements were performed on a MicroCal differential scanning calorimeter (MicroCal, Northampton, MA) with a cell volume of 0.5072 ml. All samples were degassed for 15 min at room temperature prior to scanning. Baseline scans were collected with buffer in both the reference and sample cells and later subtracted from sample scans. Proteins samples (0.2 mg/ml) in 50 mM TRIS-HCl, pH 7.5, were scanned in the temperature range 25 to 105 °C at a rate of 1 °C/min. The reversibility of the calorimetric traces was assessed by the reproducibility of scans upon rapid cooling to 25 °C followed by rescanning. To investigate whether Ca^{2+} ions had any effect on the stability of the different recombinant proteins, samples were scanned in the presence of either 5 mM EDTA or 5 mM $CaCl_2$ prepared in the same buffer.

Activity assays and thermal inactivation

Xylanase activity was determined by measuring the release of reducing sugars employing a modified version of the 3,5-dinitrosalicylic acid (DNS) stopping method described elsewhere (Nordberg Karlsson et al. 1998b), and originally reported by Miller (Miller et al. 1960). Enzyme assays were performed at 65 °C for 1 min in either 50 mM sodium phosphate buffer, pH 7.5, or in the same buffer in the presence of 5 mM EDTA where stated using 1% (w/v) of either oat spelt xylan (Sigma), birch wood xylan (Birch 7500; Roth, Karlsruhe, Germany), or β-1,3-xylan. The measurements were carried out in glass tubes containing 0.9 ml substrate, to which 100 μl sample, standard, or buffer were added. Reactions were stopped by adding 1.5 ml DNS reagent and boiling for 15 min. Standard curves were prepared under the same assay conditions using xylose as a standard, and protein concentrations used in the assay were approximately 1 μM for all the different xylanase constructs. The assay was carried out in quadruples in the case of standard curves, whereas up to six replicates were analyzed in the thermal deactivation studies.

Additional thermal inactivation assays were performed in 50 mM TRIS-HCl pH 7.5 (at 90 °C) without any additions, or in the presence of either 0.25 mM $CaCl_2$ or 5 mM $CaCl_2$. For the thermal inactivation protein samples of similar concentrations (1 μM) were used. Samples were incubated at 90 °C for different intervals, chilled on ice, and subsequently assayed as above. The inactivation kinetics of the different constructs was analyzed assuming a first-order reaction rate and using birch wood xylan as a substrate. For a constant temperature,

$$A/A_0 = e^{(-k\times t)} \quad (1)$$

$$\ln(A) - \ln(A_0) = -k \times t \quad (2)$$

where A_0 is the initial xylanase activity expressed in U/nmol protein, A is the xylanase activity at time t, expressed as above, t (min) is the time, and k is the inactivation rate constant (min^{-1}). An activity unit (U) is defined as μmol released reducing sugar ends/min. The linear regression line of the natural logarithm of the residual activity versus incubation time and the errors in the slopes were obtained using Origin General Scientific v.4.1 (Microcal Software, Northampton, MA).

To investigate whether any side-chain hydrolyzing activity resides in the full-length enzyme or its catalytic module, the arabinofuranosidase and acetyl esterase activities were assayed. The acetyl esterase activity was assayed as reported by Poutanen with some modifications using α-naphthyl acetate dissolved in dimethyl formamide (Poutanen and Sundberg 1988). Full-length Xyn10A, CM, or CBM4-2 (negative control) concentrated stocks were diluted into a 50 mM citrate-phosphate buffer, pH 6.0, containing 1 mM α-naphthyl acetate substrate up to a volume of 1 ml, and incubated at 65 °C for 20 min. This was followed by the addition of 0.5 ml of the coloring reagent (0.01% w/v Fast Corinth Salt V in 1 mM sodium acetate buffer, pH 4.3, containing 10% v/v Tween 20), and reading the absorbance at 535 nm after an additional 10 min. The arabinofuranosidase activity was assayed using a modified published protocol using *p*-nitrophenyl α-L-arabino-furanoside (*p*NP-ara; Debeche et al. 2002). The release of *p*-nitrophenol was monitored at 401 nm after adding enzyme aliquots of 100–900 μl of 1 mM *p*NP-ara in sodium acetate buffer, pH 6.0, and incubating at 65 °C for 20 min.

Results

Production and purification

The expression levels of the full-length xylanase and its deletion mutants varied from being moderately high to

high with two exceptions. The construct D3CM, comprising the third domain and the catalytic module, was poorly expressed as judged from the SDS-PAGE gel (data not shown). Concerning the third domain D3, there was hardly any visible expression product on the SDS-PAGE gel (data not shown), therefore no further work could be conducted on this construct. Furthermore, the SDS-PAGE gels and activity staining showed that the sizes of the produced proteins were in agreement with the theoretically expected, and that all variants encompassing the catalytic module displayed xylanolytic activity. Limited cleavage of the full-length xylanase Xyn10A, D3CM, and CMD5 was detected on zymograms as weak activity bands of lower molecular weight than the intact constructs (data not shown). Molecular mass analysis of the bands suggested that cleavage likely occurred in the two linker regions separating the CM from D3 and D5. The affinity chromatography purification of produced constructs was rather straightforward except for D3CM, which failed to bind to the IMAC column. This construct was, nevertheless, obtained in sufficiently pure form (approximately 90%) as described in the Materials and methods.

Activity profile

A single-point determination of initial activity of the different xylanase constructs was carried out using birch wood xylan as well as oat spelt xylan. The results are shown in Table 2. No major activity differences could be noted for the different constructs on birch xylan except for the D3CM construct, which had lower specific activity than the rest of the constructs. The same profile was noted using oat spelt xylan with D3CM showing slightly lower activity than Xyn10A and CM, but in this case the CMD5 variant exhibited even lower activity on this substrate. In the presence of EDTA, the activities of Xyn10A and CM were rather similar, but were slightly higher than in the absence of EDTA. No arabinofuranosidase, acetyl esterase, or β-1,3-xylanase activities could be detected using Xyn10A.

Table 2 The activity assays were carried out at 65 °C using equal molar concentrations of the studied proteins in 50 mM sodium phosphate buffer (*B*). For the Xyn10A and CM constructs, additional studies were carried out in the same buffer but in the presence of 5 mM EDTA (*B* + *EDTA*). The activities are reported as averages with their standard deviations. (*ND* Not determined)

Construct	Initial xylanase activity (U/nmol)		
	Birch xylan		Oat spelt xylan
	B	B + EDTA	B
Xyn10A	6.0 ± 0.7	7.7 ± 1.1	9.4 ± 0.5
D3CM	4.7 ± 0.3	ND	8.1 ± 0.3
CM	7.2 ± 0.5	7.5 ± 0.3	9.6 ± 1.3
CMD5	6.5 ± 0.3	ND	6.4 ± 0.7

Stability and calcium: DSC

To explore the thermal stability of the different xylanase variants, DSC was employed. In addition, the possible effect of calcium on the thermostability of the different mutants was investigated by conducting DSC runs in the presence of either Ca^{2+} or EDTA. The calorimetric traces were either completely irreversible or showed very little reversibility as judged from the relative area recovery, seen on the second scan. In line with our previous studies on the isolated CBMs (Abou-Hachem et al. 2002), the presence of Ca^{2+} led to decreased reversibility and seemed to aid aggregation. A summary of the T_m values obtained for the different constructs at different calcium loads is given in Table 3. In the presence of 5 mM EDTA under the experimental conditions reported, the protein is believed to exist predominantly in the apo-form (calcium-free form). Three fairly resolved thermal transitions are observed starting from 62.3 °C up to 92 °C (Fig. 2B). The middle temperature transition (73.6 °C) is broad and asymmetrical suggesting possible overlap of more than one thermal process. The thermogram of the same construct without any additions, but with no efforts done for calcium removal, is qualitatively similar in terms of the number of transitions and their shape. The first two transitions in this case are shifted toward higher temperatures, while transition 3 essentially coincides with the corresponding one in the putative apo-form of the protein (Table 3). In the third case, where a large excess of Ca^{2+} is present, the unfolding of the enzyme is characterized by a merging of the multiple transitions observed under calcium-deprived conditions into a single peak having roughly the same T_m as transition 3 in the above two cases (Table 3). These results suggest that the different

Table 3 Summary of the DSC data of Xyn10 and its deletion mutants. Samples in 10 mM TRIS-HCl, pH 7.5, were scanned without any additions (*B*), in the presence of 5 mM $CaCl_2$ in the same buffer ($B + Ca^{2+}$), or in the presence of 5 mM EDTA ($B + EDTA$). The T_m values 1, 2, and 3 represent multiple thermal transitions. For constructs CM and CMD5, where only one transition was observed, the T_m values were placed under *3* to illustrate the agreement between these values and the ones obtained for the rest of the constructs

Construct	Condition	T_m (°C)		
		1	2	3
Xyn10A	B	71.6	85.8	91.9
	B + Ca^{2+}	–	–	93.0
	B + EDTA	62.3	73.6	92.0
D3CM	B	69.0	–	89.8
	B + Ca^{2+}	–	–	89.5
	B + EDTA	60.6	–	89.8
CM	B	–	–	88.8
	B + Ca^{2+}	–	–	89.5
	B + EDTA	–	–	88.3
CMD5	B	–	–	88.7
	B + Ca^{2+}	–	–	88.4
	B + EDTA	–	–	88.9

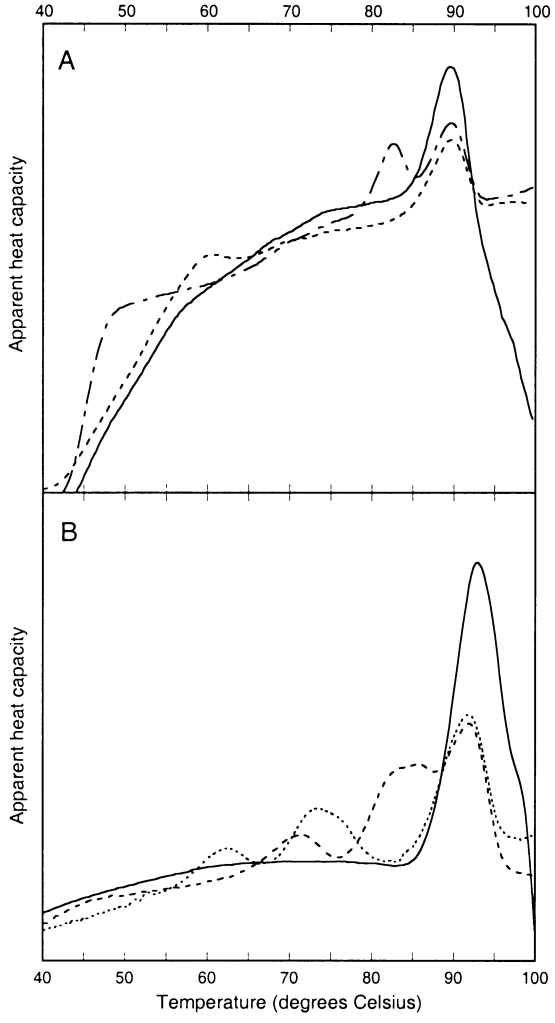

Fig. 2A, B Differential scanning calorimetry thermograms of the two Xyn10A constructs. **A** D3CM without any additions (*dashed line*), D3CM in the presence of 0.5 mM $CaCl_2$ (*long and short dashed line*), and D3CM in the presence of 5 mM $CaCl_2$ (*solid line*). The two thermal transitions observed when scanning samples with partial calcium occupancy (*dashed curves*) merge into a single transition in the presence of 5 mM calcium (*solid curve*). **B** Xyn10A in the presence of 5 mM EDTA (*dotted line*), Xyn10A without any additions (*dashed line*), and Xyn10A in the presence of 5 mM $CaCl_2$ (*solid line*). Presence of calcium leads to the merging of different transition into a cooperative unfolding peak

transitions observed are associated with the unfolding of discrete modules or domains in the enzyme. Transition 3 is unaffected by Ca^{2+} whereas transitions 1 and 2 show considerable calcium dependence. This implies that the modules or domains connected to the calcium-dependent transitions, bind Ca^{2+} in a specific fashion, thus elevating their unfolding temperatures. This conclusion finds support in our earlier studies, which established that both Xyn10A CBMs bind calcium ions, increasing their unfolding temperatures (Abou-Hachem et al. 2002). By contrast, the CM and CMD5 constructs were unaffected by Ca^{2+} ions (Table 3), ruling out any specific calcium binding roles of both the catalytic module and the fifth domain. Hence, D3 seems to be the more plausible domain for the divalent ligand binding besides the N-terminal CBMs. This is indeed in conformity with DSC scans carried out on the D3CM construct. The same trend of T_m of the lower transitions shifting to higher temperatures with increasing Ca^{2+}, and subsequently merging with transition 3 is shared between Xyn10A and D3CM (Fig. 2). These results strongly suggest the third domain to be involved in specific calcium binding. For the putative apo-form of the D3CM construct comprising the third domain and the catalytic module, transitions 1 and 3 are likely to be linked to the unfolding of the third domain and the catalytic module, respectively. Explicit evidence for this could not be provided as no studies could be conducted on the isolated third domain. However, the thermograms of the isolated catalytic module (CM) strengthen this claim as the only transition obtained in that case agrees well with transition 3 for the D3CM construct (Table 3). Comparing the thermograms of the Xyn10A and the D3CM constructs in the putative apo-form, shows that the T_m values of transition 1 in both cases are fairly similar (60.6 and 62.3 °C for D3CM and Xyn10A, respectively). This leads us to conclude that in the apo-form, the first step in the denaturation of the full-length Xyn10A may be the unfolding of the third domain, possibly along with CBM4-1 which shows two transitions at 63.2 and 76 °C under the same conditions (unpublished data).

Stability and calcium: thermal inactivation

Two different buffer systems were used for the inactivation studies: phosphate buffer which has very little pH-temperature dependence but has the disadvantage of calcium incompatibility, building precipitates with calcium ions, and TRIS-HCl buffer which displays no interference with calcium, but for which temperature-induced changes in its pK_a value must be compensated. Kinetic stability of the different xylanase variants was compared under calcium-deprived conditions (in the presence of 5 mM EDTA), under partial calcium saturation (without any Ca^{2+} additions, but with no efforts made to remove residual bound calcium in both TRIS-HCl and phosphate buffers), and in the presence of calcium (0.25 or 5 mM Ca^{2+} in TRIS-HCl buffer). The results are summarized in Table 4. In the presence of 5 mM Ca^{2+} in TRIS-HCl buffer, the activity of the full-length enzyme decreased substantially after 5 min indicative of aggregation, and no inactivation rate constant could be determined. Lowest stability of Xyn10A was measured in the same buffer when 0.25 mM Ca^{2+} was added. By contrast, the full-length xylanase showed best stability in TRIS-HCl without any additions, approximately twofold better than under the same conditions in phosphate buffer. In phosphate buffer, the full-length xylanase showed a 34% decreased stability in the presence of EDTA as compared to the enzyme without any additions. These results suggest that high affinity calcium binding is likely to be responsible for this stabilization. The differ-

Table 4 The inactivation studies were carried out at 90 °C using equal molar concentrations of the studied proteins in 50 mM sodium phosphate buffer (*B*) or 50 mM TRIS-HCl (*B**). For the Xyn10A and CM constructs, additional studies were carried out in the same buffer but in the presence of 5 mM EDTA (*B + EDTA*), and for Xyn10A also in the presence of 0.25 mM Ca^{2+}. (*ND* Not determined)

Construct	Inactivation rate constant $k(min^{-1})$			
	B	B + EDTA	B*	B* + Ca^{2+}
Xyn10A	$(13 \pm 1.2)\times10^{-3}$	$(19.9 \pm 1.2)\times10^{-3}$	$(5.7 \pm 0.7)\times10^{-3}$	$(27.2 \pm 5)\times10^{-3}$
D3CM	$(18.4 \pm 1.1)\times10^{-3}$	ND	ND	ND
CM	$(17.7 \pm 0.6)\times10^{-3}$	$(16.9 \pm 0.7)\times10^{-3}$	ND	ND
CMD5	$(17.2 \pm 1)\times10^{-3}$	ND	ND	ND

ence in kinetic stability between the forms of the catalytic module with or without EDTA was marginal in the same buffer, excluding destabilization by EDTA or unspecific stabilization by calcium ions solely as credible causes for the stability difference observed in the case of the full-length enzyme. Considering the stability of the full-length enzyme as compared to its deletion mutants, our data in phosphate buffer show that all the truncated forms of the enzyme displayed decreased thermostability, with the D3CM construct being the least stable.

Discussion

The modular thermostable xylanase from *Rhodothermus marinus* has been subject to several studies during recent years, in which focus primarily has been set on function and biochemical/biophysical properties of its individual modules (Abou Hachem et al. 2000; Nordberg Karlsson et al. 1998a, b). A recent study on the second isolated CBM (CBM4-2) showed that the thermostability of that module (as well as CBM4-1) was strongly dependent on the presence of calcium ions (Abou-Hachem et al. 2002). CBM4-2 specifically binds two calcium ions, one with moderate ($k_a \approx 10^5\ M^{-1}$, where k_a is the association constant) and the other with extremely high affinity ($k_a \approx 10^{10}\ M^{-1}$) which stabilizes the overall fold of the module (Abou-Hachem et al. 2002; Simpson et al. 2002). The stabilizing effect of the specific calcium-binding on the CBMs was much more pronounced than the stabilizing effect of substrate, which for the CM was shown to increase the T_m a few degrees (Pfabigan et al. 2002). The main objective of this study was to analyze whether the thermostability of the full-length xylanase was dependent on specific calcium binding, and whether additional calcium binding sites besides those found in the N-terminal CBMs existed. For this purpose, several truncated forms of the xylanase were designed for expression and characterization. DSC, a technique proved to be powerful when investigating multidomain proteins (Ruiz-Arribas et al. 1994; Sturtevant 1987), was employed to assess thermostability of the Xyn10A variants. The low reversibility of the calorimetric traces, commonly seen for large modular proteins, however hindered quantitative analysis of the obtained thermograms. This was especially pronounced in the presence of Ca^{2+}, which aided aggregation, in line with the observations on the effect of the same ion on CBM4-2 (Abou-Hachem et al. 2002). Nevertheless, the thermograms and T_m values yielded convincing evidence that calcium ions had a pronounced effect on the thermostability of Xyn10A. It was also shown that, in addition to the N-terminal CBMs, the third domain (D3) binds Ca^{2+}, resulting in a large increase of approximately 29 °C in the unfolding temperature (Table 2). Although the stoichiometry of calcium binding has not been established for Xyn10A, our data strongly suggest D3 to possess both a high and a moderate/weak affinity binding site. The presence of a putative high affinity site is supported by the observation that addition of EDTA to D3CM lowered the T_m of transition 1 (plausibly representing D3 unfolding) by approximately 9 °C (Table 3). Hence, calcium was extracted from a site saturated by the residual Ca^{2+} ion concentration in the low micromolar range always present in buffers (if no special efforts are made for its removal) that are sufficient to saturate high affinity binding sites ($k_a >> 10^6\ M^{-1}$) in proteins. In addition, at least one moderate/weak affinity binding site ($k_a < 10^6\ M^{-1}$) seems to be present as the addition of 0.5 mM Ca^{2+} to the same construct was not sufficient for saturation (Fig. 2A). Different thermal unfolding pathways can thus be suggested for the putative apo-form and the calcium-loaded form of Xyn10A. In the apo-form, unfolding most likely starts with D3 and CBM4-1 followed by CBM4-2 and finally the catalytic module and D5. In the calcium-loaded form, which is likely to contain up to six calcium ions, Xyn10A displays cooperative unfolding seen as a single high temperature transition. The enzyme-stabilizing role played by high affinity bound calcium ions is reinforced by the thermal inactivation data, since highest kinetic stability was observed in TRIS-HCl buffer followed by phosphate buffer (Table 4; Fig. 3). Under both the above conditions the high affinity sites are most likely saturated, and the better stability in TRIS-HCl, as compared to phosphate, is consistent with the fact that PO_4^{3-} ions build precipitate with Ca^{2+}, resulting in lower free calcium available for the enzyme. Although a large excess of calcium enhanced the thermodynamic stability of the enzyme (Table 3), the kinetic stability decreased considerably. This is most likely due to aggregation, a hypothesis supported by inactivation

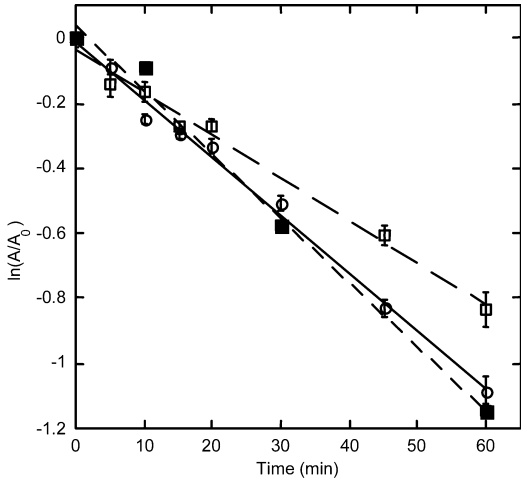

Fig. 3 The displayed curves represent thermal inactivation experiments carried out at 90 °C in 50 mM phosphate buffer pH 7.5 assayed using birch xylan as a substrate. The full-length xylanase in phosphate buffer (*open squares*) displayed highest stability in comparison with the same construct in the presence of 5 mM EDTA (*filled squares*) and the isolated catalytic module (*open circles*). *Data points* are the means of up to six replicates and *error bars* denote the standard error of the means (SEM). *Straight lines* joining the data are linear fits generated using KaleidaGraph v.3.5

studies at even higher Ca^{2+} concentrations (5 mM), in which severe aggregation occurred. Best kinetic stability was thus displayed at an optimal low calcium concentration, where the high affinity and possibly moderate affinity sites were occupied, but with no excess free calcium.

Another observation noted from inactivation rate constants comparison is the higher stability of the full-length enzyme than of its three deletion mutants lacking the N-terminal CBMs. This suggests module/domain interactions to be contributing to the stability, but to a limited extent, as their contributions do not appear to be crucial for stability (Table 4). The notion that thermostabilization is the major advantage of having CBMs or other domains attached to glycoside hydrolase catalytic modules (or the very existence of exclusively thermostabilizing domains) has recently been questioned (Charnock et al. 2000; Sunna et al. 2000), which is in line with the results presented here. Different degrees of module–module interaction have also emerged from the very few structures of modular GHs that have been solved, varying from no interaction at all to very tight interactions resulting in rigid well-defined entities. The first structure of a cellulase (GHF 9) and an intact CBM (family 3c) showed that the two-module fragment had a rigid structure with the active site of the CM and the substrate binding surface of the CBM aligned (Sakon et al. 1997). A markedly diminished activity and thermostability, after deletion of the CBM, also reflected this intimate and spatially defined interaction (Irwin et al. 1998). Similar intimate association and alignment of binding faces have been shown between a chitin-binding module and chitinase CM, although the modules in this case are separated by a long but inflexible linker that runs along the surface of the catalytic module (van Aalten et al. 2000). The crystal structure of the GHF 10 xylanase from *Streptomyces olivaceoviridis* E-86 and its xylan binding module (XBM), on the other hand, revealed the two modules to be connected by a highly mobile linker. These modules make contacts along their hydrophilic interface, but in a less extensive manner, the binding surfaces are not aligned, and module movement is proposed to explain the mode of action of the enzyme (Fujimoto et al. 2000). Proteolysis patterns during production of *Rm*Xyn10A and its variants indicate that cleavage only occurs between D3 and the catalytic module and between the latter and D5, implying these linkers to be more flexible and exposed than the one separating the two CBMs. It is tempting to speculate whether the heterogeneity (for example, in side chain substitution) and helical conformation of xylan-based substrates favor more flexible connections between CMs and adjacent domains/modules, as compared to crystalline cellulose/chitin hydrolyzing CMs, for which rigid aligned CBMs may offer a considerable extension of the substrate binding site.

Studies conducted up to date have failed to unravel the function of the two domains, D3 and D5, in Xyn10A. Interestingly, the C-terminal domain (D5) shares significant primary structure similarity with the C-terminal part of a GHF 26 mannanase (33% identity) originating from the same organism. A multisequence alignment of the catalytic modules of GHF 26 suggests this C-terminal part of the mannanase to be a separate domain as it flanks the CMs downstream of the consensus region, rather than lying within it (data not shown). Affinity electrophoresis analysis, however, failed to show any mannan-binding capacity (data not shown), which ruled out a mannan-binding function. It has been suggested that the *R. marinus* mannanase is cell bound (Politz et al. 2000) and the C-terminal domain which resembles D5 in Xyn10A is then a likely candidate to mediate the cell attachment. A similar function can not be excluded in the case of Xyn10A, although additional studies are required to assess the validity of this claim.

The third domain (D3) did not share sequence similarity with other reported sequences, and no substrate binding or side-chain hydrolyzing function could be demonstrated on tested substrates (data not shown). Failure to express the isolated D3, and low expression levels, lower initial activity, and lower thermal stability of the construct D3CM may suggest conformational instability or improper folding when the CBMs preceding this domain were deleted. Moreover, the produced D3CM failed to bind to the immobilized Cu^{2+} in the IMAC column, which makes it likely that D3 adopted a conformation with respect to the catalytic module (for example, back to back stacking), such that the C-terminal histidine tag is inaccessible. This is conceivable as the linker between D3 and the catalytic module is the longer ($\approx$17–19 amino acid residues) of the three linkers identified in the xylanase (Fig. 1), which offers conformational freedom assuming linker flexibility. We

have shown that D3 binds at least one calcium ion with high affinity, resulting in a thermostabilizing effect on the whole modular xylanase. Calcium ions play diverse roles in biological systems and their thermostabilizing role in proteins has frequently been investigated (Evenäs et al. 1998; Linse and Forsen 1995). Except for amylases, the reports on calcium binding to glycoside hydrolases are relatively few. To the best of our knowledge there is only one GHF 10 xylanase that binds calcium in an inserted loop in the $(\alpha/\beta)_8$ barrel structure (Spurway et al. 1997). By contrast, it is now established that calcium binding is a conserved property within some CBM families (Abou-Hachem et al. 2002; Charnock et al. 2000; Czjzek et al. 2001; Tormo et al. 1996). This is the first report on the stabilizing role of calcium on a modular GHF 10 xylanase via multiple binding to its both CBMs and to a third domain of unknown function. Unraveling the function and structure of this calcium-binding domain would add to our understanding of the molecular architecture of this enzyme, and therefore additional studies to achieve this goal are motivated.

Acknowledgments We want to thank Professor T. Araki for providing 1–3 linked xylan. We would like to express gratitude to the Swedish Research Council (VR) and the Royal Physiographic Society in Lund for financial support.

References

Abou Hachem M, Nordberg Karlsson E, Bartonek-Roxa E, Raghothama S, Simpson PJ, Gilbert HJ, Williamson MP, Holst O (2000) Carbohydrate-binding modules from a thermostable *Rhodothermus marinus* xylanase: cloning, expression and binding studies. Biochem J 345:53–60

Abou-Hachem M, Nordberg Karlsson E, Simpson PJ, Linse S, Sellers P, Williamson MP, Jamieson SJ, Gilbert HJ, Bolam DN, Holst O (2002) Calcium binding and thermostability of carbohydrate binding module CBM4–2 of Xyn10A from *Rhodothermus marinus*. Biochemistry 41:5720–5729

Alfredsson GA, Kristjansson JK, Hjörleifsdottir S, Stetter KO (1988) *Rhodothermus marinus*, gen. nov., sp. nov., a thermophilic, halophilic bacterium from submarine hot springs in Iceland. J Gen Microbiol 134:299–306

Charnock SJ, Bolam DN, Turkenburg JP, Gilbert HJ, Ferreira LM, Davies GJ, Fontes CM (2000) The X6 "thermostabilizing" domains of xylanases are carbohydrate-binding modules: structure and biochemistry of the *Clostridium thermocellum* X6b domain. Biochemistry 39:5013–5021

Coutinho PM, Henrissat B (1999) Carbohydrate-active enzymes: an integrated database approach. In: Gilbert HJ, Davies GJ, Henrissat B, Svensson B (eds) Recent advances in carbohydrate bioengineering. The Royal Society of Chemistry, Cambridge, pp 3–12

Czjzek M, Bolam DN, Mosbah A, Allouch J, Fontes CM, Ferreira LM, Bornet O, Zamboni V, Darbon H, Smith NL, Black GW, Henrissat B, Gilbert HJ (2001) The location of the ligand-binding site of carbohydrate-binding modules that have evolved from a common sequence is not conserved. J Biol Chem 276:48580–48587

Debeche T, Bliard C, Debeire P, O'Donohue MJ (2002) Probing the catalytically essential residues of the alpha-L-arabinofuranosidase from *Thermobacillus xylanilyticus*. Protein Eng 15:21–28

Evenäs J, Malmendal A, Fors'en S (1998) Calcium. Curr Opin Chem Biol 2:293–302

Fujimoto Z, Kuno A, Kaneko S, Yoshida S, Kobayashi H, Kusakabe I, Mizuno H (2000) Crystal structure of *Streptomyces olivaceoviridis* E-86 beta-xylanase containing xylan-binding domain. J Mol Biol 300:575–585

Gilbert HJ, Hazlewood GP (1993) Bacterial cellulases and xylanases. J Gen Microbiol 139:187–194

Henrissat B, Teeri TT, Warren RA (1998) A scheme for designating enzymes that hydrolyse the polysaccharides in the cell walls of plants. FEBS Lett 425:352–354

Irwin D, Shin DH, Zhang S, Barr BK, Sakon J, Karplus PA, Wilson DB (1998) Roles of the catalytic domain and two cellulose binding domains of *Thermomonospora fusca* E4 in cellulose hydrolysis. J Bacteriol 180:1709–1714

Joseleau JP, Comtat J, Ruel K (1992) Chemical structure of xylans and their interaction in the plant cell walls. In: Visser J, Beldman G, Kusters-van Someren MA, Voragen AGJ (eds) Xylans and xylanases. Elsevier, Amsterdam, pp 1–15

Linse S, Forsen S (1995) Determinants that govern high-affinity calcium binding. Adv Second Messenger Phosphoprotein Res 30:89–152

Miller GL, Blum R, Glennon WE, Burton AL (1960) Measurement of carboxymethylcellulase activity. Anal Biochem 2:127–132

Nordberg Karlsson E, Bartonek-Roxå E, Holst O (1997) Cloning and sequence of a thermostable multidomain xylanase from the bacterium *Rhodothermus marinus*. Biochim Biophys Acta 1353:118–124

Nordberg Karlsson E, Bartonek-Roxa E, Holst O (1998a) Evidence for substrate binding of a recombinant thermostable xylanase originating from *Rhodothermus marinus*. FEMS Microbiol Lett 168:1–7

Nordberg Karlsson E, Dahlberg L, Torto N, Gorton L, Holst O (1998b) Enzymatic specificity and hydrolysis pattern of the catalytic domain of the xylanase Xynl from *Rhodothermus marinus*. J Biotechnol 60:23–35

Painter TJ (1983) Algal polysaccharides. In: Aspinall GO (ed) The polysaccharides. Academic, London, pp 195–285

Pfabigan N, Nordberg Karlsson E, Ditzelmueller G, Holst O (2002) Prebleaching of kraft pulp with full-length and functional domains of a thermostable xylanase from *Rhodothermus marinus*. Biotechnol Lett 24:1191–1197

Politz O, Krah M, Thomsen KK, Borriss R (2000) A highly thermostable endo-1,4-beta-mannanase from the marine bacterium *Rhodothermus marinus*. Appl Microbiol Biotechnol 53:715–721

Poutanen K, Sundberg M (1988) An acetyl esterase of *Trichoderma reesei* and its role in the hydrolysis of acetyl xylans. Appl Microbiol Biotechnol 28:419–424

Ramchuran SO, Nordberg Karlsson E, Velut S, de Maré L, Hagander P, Holst O (2002) Production of heterologous thermostable glycoside hydrolases and the presence of host-cell proteases in substrate limited fed-batch cultures of *Escherichia coli* BL21(DE3). Appl Microbiol Biotechnol 60:408–416

Ruiz-Arribas A, Santamaria RI, Zhadan GG, Villar E, Shnyrov VL (1994) Differential scanning calorimetric study of the thermal stability of xylanase from *Streptomyces halstedii* JM8. Biochemistry 33:13787–13791

Sakon J, Irwin D, Wilson DB, Karplus PA (1997) Structure and mechanism of endo/exocellulase E4 from *Thermomonospora fusca*. Nat Struct Biol 4:810–818

Simpson PJ, Jamieson SJ, Abou-Hachem M, Nordberg Karlsson E, Gilbert HJ, Holst O, Williamson MP (2002) The solution structure of the CBM4–2 carbohydrate binding module from a thermostable *Rhodothermus marinus* xylanase. Biochemistry 41:5712–5719

Spurway TD, Morland C, Cooper A, Sumner I, Hazlewood GP, O'Donnell AG, Pickersgill RW, Gilbert HJ (1997) Calcium protects a mesophilic xylanase from proteinase inactivation and thermal unfolding. J Biol Chem 272:17523–17530

Sturtevant JM (1987) Biochemical applications of differential scanning calorimetry. Annu Rev Phys Chem 38:463–488

Sunna A, Gibbs MD, Bergquist PL (2000) The thermostabilizing domain, XynA, of *Caldibacillus cellulovorans* xylanase is a xylan binding domain. Biochem J 346:583–600

Tomme P, Warren RAJ, Gilkes NR (1995) Cellulose hydrolysis by bacteria and fungi. In: Poole RK (ed) Advances in microbial physiology. Academic, London, pp 2–81

Tormo J, Lamed R, Chirino AJ, Morag E, Bayer EA, Shoham Y, Steitz TA (1996) Crystal structure of a bacterial family-III cellulose-binding domain: a general mechanism for attachment to cellulose. EMBO J 15:5739–5751

Van Aalten DM, Synstad B, Brurberg MB, Hough E, Riise BW, Eijsink VG, Wierenga RK (2000) Structure of a two-domain chitotriosidase from *Serratia marcescens* at 1.9-Å resolution. Proc Natl Acad Sci U S A 97:5842–5847

Warren RA (1996) Microbial hydrolysis of polysaccharides. Annu Rev Microbiol 50:183–212

Wicher KB, Abou-Hachem M, Halldorsdottir S, Thorbjarnadottir SH, Eggertsson G, Hreggvidsson GO, Nordberg Karlsson E, Holst O (2001) Deletion of a cytotoxic, N-terminal putative signal peptide results in a significant increase in production yields in *Escherichia coli* and improved specific activity of Cel12A from *Rhodothermus marinus*. Appl Microbiol Biotechnol 55:578–584